ORIGINAL CONTRIBUTION

WILEY | JCD Journal of Cosmetic Dermatology

From stem cells protection to skin microbiota balance: *Orobanche rapum* extract, a new natural strategy

Marie Meunier MD[1] (iD) | Amandine Scandolera PhD[1] | Emilie Chapuis BD[1] |
Carole Lambert PhD[2] | Cyrille Jarrin PhD[2] | Patrick Robe PhD[2] | Hanane Chajra PhD[2] |
Daniel Auriol PhD[2] | Romain Reynaud MD[1]

[1]Research and Development, Givaudan France SAS, Pomacle, France

[2]Research and Development, Givaudan France SAS, Toulouse, France

Correspondence
Marie Meunier, Givaudan Active Beauty, Pomacle, France.
Email: marie.meunier@givaudan.com

Summary

Background: Healthy skin is a delicate balance between skin renewal and microbiota homeostasis, and its imbalance promotes premature aging and dermatological disorders. Skin stem cells are key actors in this process but their sensitivity to aging and external stressors such as UV reduces the skin renewal power. The skin microbiota has been recently described as active in the healthy skin, and its imbalance could trigger some disorders.

Aims: We hypothesized that reactivation of stem cells and maintenance of microbiota could be a disruptive strategy for younger and healthier skin. We thus developed a new plant extract that restores the entire skin renewal process by sequential activation from stem cells stimulation to microbiota protection.

Methods: We studied stem cells comportment in the presence of *Orobanche rapum* extract by survivin immunocytochemistry and caspases 3 and 9 dosages. We also analyzed epidermal differentiation markers by immunohistochemistry and lipids organization by GC/MS At the clinical level, we investigated the impact of *O. rapum* extract on microbiota and on skin aspect.

Results: We demonstrated an active protection of skin stem cells through the maintenance of their clone-forming capacity and resistance to UV through the overexpression of survivin coupled to caspases inhibition. Furthermore, we showed the restoration of epidermal differentiation markers and ceramide biosynthesis favorable to orthorhombic organization. Clinical studies, including microbiota analysis, showed an active skin surface renewal coupled with microbiota protection.

Conclusion: We evidenced that our active ingredient is able to stimulate skin rejuvenation while protecting the cutaneous microbiota, creating healthier skin and thereby beauty.

KEYWORDS

microbiota, *Orobanche rapum*, rejuvenation, skin health, stem cells

1 | INTRODUCTION

Skin is one of the body's biggest and most important organs, due to its role in protecting against external aggressors. To serve this function durably, it is important to maintain skin health; this can be wined through a combination of skin renewal and microbiota homeostasis properties.

The first component of the skin renewal process is a reservoir of stem cells in the basal layer of the epidermis. These cells have self-renewal potential that allows them to remain sufficiently numbered in the epidermis. This is achieved through symmetrical division. The cells are also able to divide asymmetrically, in that case they produce an identical cell and somewhat a differentiated daughter. These two types of division ensure maintenance of a pool of stem cells, while also renewing skin tissue.[1,2] Skin stem cells are rare and secured in niches with a specific protective microenvironment which can be troubled and destabilized by exposure to ultraviolet (UV) radiation.[3] UV radiation also induces a decrease in stem cell colony-forming potential,[4] leading to premature extrinsic aging through a degradation of the stem cells' integrity. Intrinsic aging, however, is not without consequences: aging stem cells can lose their ability to differentiate in progenitor or effector cells and their self-renewal capabilities can decline. As a result, they decrease in number, leading to a skin-specific aging phenotype.[5,6] Fortunately, stem cells possess a self-defense mechanism called survivin. Survivin is a biomarker specific to stem cells which has different biological functions according to its location. Whereas when located in a nucleus, survivin allows the pool of stem cells to be maintained by controlling cell division, this is not the case when it is located in mitochondria and released to the cytoplasm. In the latter case, it inhibits caspases 3 and 9 to keep stem cells in survival.[7]

These protected stem cells are differentiated from the other cells in the basal layer through their high expression of integrin β1, another specific marker of epidermal stem cells.[8] The other keratinocytes in the basal layer have a limited number of division cycles and lose their ability to adhere to the basal layer and differentiate into cells from the spinous layer.[9] At this state of differentiation, keratinocytes present a specific polyhedral morphology due to the contraction of microfilament between desmosomes. When spinous cells differentiate in granular cells in the top layer, they form keratohyalin granules inside their cytoplasm. These are composed of the keratin filaments profilaggrin and loricrin. Granular cells are also composed of lamellar bodies which allow for the accumulation of the lipids within. These keratinocytes form a granular layer and then start to lose their nucleus and cytoplasmic organelles, which release mature filaggrin, aggregating with keratin filaments and forming a cornified cell envelope.[10] They then seal together in several layers to form a physical barrier, expressing specific markers of the terminal epidermal differentiation: filaggrin, loricrin, and involucrin. At the state of *stratum corneum*, these cohesive cells called corneocytes produce lipids such as cholesterol, free fatty acids, and ceramides, which are composed of a sphingoid part of 18 carbon atoms—sphingosine, dihydrosphingosine, and phytosphingosine—covalently bound to a fatty acid itself part of 16-24 carbons atoms—nonhydroxy and α-hydroxy fatty acids.[11] The long chain length of ceramides improves the orthorhombic organization of lipids, constituting a matrix embedding corneocytes. This forms a structure of "brick and mortar" which offers the skin a physical barrier with water-holding properties.[12]

When skin is entirely renewed, from its stem cells to its *stratum corneum*, the last step to complete skin renewal is the process of desquamation. This desquamation process normally occurs every two to four weeks. Every layer is replaced by a new one, and so a new *stratum granulosum* is formed below the ancient *stratum corneum*. Lamellar bodies present in stratum granulosum cells contain kallikrein 5 (KLK5), a serine protease which is pH sensitive and activates in environments with acidic pH, as is the case in the *stratum corneum*.[13] This protease, specialized in cleavage of corneodesmosome components, is then activated, leading to the desquamation process.[14] *Stratum corneum* gradually loses its cohesion until total detachment occurs from the underlying layer while said layer is differentiating in a new *stratum corneum*. Kallikrein 5 is considered to be a key factor in the final desquamation process, an essential step in recycling the *stratum corneum* and preventing the accumulation of cells and debris on the skin's surface. This recycling is accompanied by a feeling of roughness and dryness.

Although it has been established that the *stratum corneum* is the upper layer of the skin, there does remain a final superficial layer called the Stratum microbium™ by Givaudan in March 2015. This layer represents the global innate population of microorganisms living on the skin's surface, and it interacts and works together with human skin cells to keep people healthy and protect them.[15] A strong and balanced microbiota is essential for health and is achieved through protection of commensal bacteria and the prevention of pathogenic bacteria proliferation.[16-18] A balanced skin microbiota offers skin an additional protection against premature aging.[19]

Orobanche rapum-genistae is a chlorophyll less plant, growing on the roots of *Cytisus scoparius*. It contains the phenylpropanoid glycosides acteoside and crenatoside.[20]

In this study, we first demonstrate in vitro how *O. rapum* extract impacts skin renewal at the stem cell level. We then show how this protection leads to the improvement of epidermal differentiation on a model of reconstructed human epidermis (RHE). The impact of *O. rapum* extract on epidermis impermeability was studied by analyzing ceramide content. Impact of the extract on skin was studied up to the process of desquamation at the ex vivo level.

At the clinical level, we ended with an evaluation of the final effect on wrinkle appearance and also studied how *O. rapum* extract modulates the skin's microbiota balance, leading to better protection.

2 | MATERIAL AND METHODS

2.1 | Plant extract

Orobanche rapum was collected by hand in France, dried and crushed. An ethanolic extraction (1 kg of plant for 6 kg of ethanol 96°C) was performed at 50°C for 4 h. Ethanol was removed under vacuum evaporator and replaced by 1,3-propanediol. The extract was decolorized on charcoal plate and filtered sterically.

2.2 | Improvement of skin rejuvenation

2.2.1 | Stem cell resistance to UV exposure

The cells used in this study were primary normal human hair follicle Outer Root Sheath cells (hORS) provided by Celprogen (Torrance, CA, USA). hORS were seeded on eight-well slides or Petri dishes (between 10 000 and 60 000 hORS/cm^2) and were left to adhere for 1-3 days at 37°C/5% CO$_2$ in complete medium. Cells were pre-treated for 24 hours with or without *O. rapum* extract at 0.5% and were or were not irradiated for 25 minutes at UVA (8 J/cm^2) and UVB (150 J/cm^2) in a saline buffer. After UV exposure, cells were treated again with or without *O. rapum* extract at 0.5% for 24 hours. Cells were incubated at 37°/5% CO$_2$ for all the treatment times, and applications were done in serum-free medium.

2.2.2 | Immunofluoresence of survivin

After the stimulation and UV exposure of hORS, cells were finally fixed with formaldehyde (4%) and were permeabilized with 0.1% Triton X-100. Unspecific fixation sites were blocked with serum from the same species as the secondary antibody (Santa Cruz, Dallas, TX, USA). After primary antibody incubation (Survivin NB500-237; Novus-Biologicals, Littleton, CO, USA) overnight at 4°C, cells were incubated with secondary antibody coupled to a fluorochrome Alexa Fluor 546 nm which is excited at 488 nm and emits signal at 546 nm (Invitrogen, ThermoFisher Scientific, Courtaboeuf, France) and DAPI (Roche, Basel, Switzerland) coloring nucleus for 2 hours at room temperature. Finally, slides were mounted with a mounting medium (DAKO, Agilent Technologies, Santa Clara, CA, USA) that provided fluorescence protection and coverslip adhesion for the materials. The fluorescence was analyzed with a fluorescence optic microscope (Olympus CK40; Olympus Corporation, Shinjuku, Tokyo, Japan) and appropriate filters to the fluorochrome. Image acquisition was performed with the software Archimed (Microvision, Redmond, WA, USA). The quantification was performed using the Colombus software (PerkinElmer, Waltham, MA, USA), as mean intensity (12 images for each condition). This was the mean value of intensity for each pixel of staining, contained in the red-stained cell area.

2.2.3 | Inhibition caspase 3 and caspase 9

Caspase 3 or caspase 9 and their specific substrate (Invitrogen) were incubated in the absence (control) or presence of reference product or of increasing concentrations of *O. rapum* extract (0.1%, 0.5% and 1%). *Orobanche rapum* extract was diluted directly in the reaction buffer. Ac-DEVD-CHO at 5 nmol/L was used as a reference inhibitor for caspase 3 enzyme. Ac-LEHD-CHO at 0.5 μmol/L was used as reference inhibitor of the caspase 9 enzyme. At the end of the incubation period (20 minutes for caspase 3 and 30 minutes for caspase 9), the product which is formed from the cleavage of the specific substrate and per caspase was measured with a luminometer (Invitrogen). Results are expressed as Relative Luminescence Unit (RLU, mean ± SD).

2.3 | Improvement of skin epidermal differentiation

2.3.1 | Reconstructed human epidermis (RHE) culture and stripping

The study was performed using reconstructed human epidermis from primary keratinocytes in a serum-free, differentiation culture medium (RHE batch RH0615/1, StratiCELL® EPI/001). The reconstructed tissues were cultivated at the air-liquid interface for 14 days in a humidified incubator at 37°C in a 5% CO$_2$ atmosphere. The epidermises were stripped on the 11th day, before addition of topically applied creams. Hyaluronic acid solubilized in the culture medium (50 μg/mL) was used as a reference molecule and incubated for 72 hours. Cream which either did or did not contain the *O. rapum* extract at 0.5% was deposited on top of the skin and incubated for 72 hours at 37°C in a 5% CO$_2$ atmosphere.

2.3.2 | Epidermal differentiation marker expression by immunofluorescence

During immunostaining, the first step was to remove the paraffin from tissue sections and place the slices in a 0.01 mol/L citrate buffer, pH 6. The slices were then washed with PBS and incubated in a saturation solution containing 5% serum for 1 hour at room temperature, then in the presence of anti-filaggrin (Acris Antibodies GmbH, Herford, Germany AM00245PU-N), anti-involucrin (Abcam, Paris, France; ab53112) and anti-loricrin primary antibodies (Abcam; ab24722), for 1 hour in a humid chamber and at room temperature. The samples were then washed twice in 0.1% PBS-Tween 20 and once in PBS before being incubated for 30 minutes in PBS in the presence of fluorescein-conjugated anti-mouse or anti-rabbit secondary antibodies. 4′, 6′-diamidino-2-phenylindole, or DAPI, a fluorescent molecule capable of binding to the adenine and thymine bases of DNA was used to detect nuclei of keratinocytes. The slices were then mounted in Mowiol (Sigma-Aldrich, St. Louis, MI, USA) medium. For each immunostaining session, three photos were captured using a Leica DM100 microscope and a DCF290 camera at 40× magnification. Image quantification was performed using the QWin 3 analysis software (Leica, Wetzlar, Germany). The detection thresholds were determined prior using the most marked slices, in order to avoid saturation of detection. For each photo, an area of interest was delimited and surface was measured. The surface corresponds to the viable layers of the epidermis with the exception of the basal layer. The software then measured the marked area within the delimited area, in number of pixels. The mean intensity of the marked surface multiplied by the ratio "marked/total surface" determines the intensity of marking for a given slice.

2.3.3 | Disrupted barrier function by cytokine cocktail on RHE

The model used was the inflammatory reconstructed human epidermis (RHE) model. This model is suitable for barrier default study. Indeed, the inflammation leading to barrier default is triggered by the cytokines mixture. The study was done in triplicate on normal

RHE (unstressed) and on RHE stressed under cytokines mixture. The RHE were prepared with keratinocytes obtained from a 24-year-old female donor. For the inflammatory RHE, the cultured protocol was the following: On day 6 of air exposure, a mix of cytokines (IL-4, IL-13, IL-17E, IL-31 and TNF-α at 15 ng/mL each) was supplemented to the medium until day 10 with and without *O. rapum* extract at 0.5%. The reference molecule used in this study was sodium butyrate at 0.1%. Normal RHE was cultured 10 days.

2.3.4 | Quantification and analysis of skin lipids

Characterization and evaluation of *O. rapum* extract efficacy were performed using a biochemical approach on lipids involved in the barrier function: polar lipids including ceramides (Sphingosine [S], Dihydrosphingosine [DS], Phytosphingosine [P] base with chain lengths of 16 and 18 carbon atoms) were analyzed by LC/MS Neutral lipids with free fatty acids, cholesterol, and glycerides were analyzed by GC/MS

2.4 | Improvement of desquamation

2.4.1 | KLK5 immunostaining from skin explants

Kallikrein 5 (KLK5) expression was analyzed by immunohistochemistry using rabbit polyclonal antibody anti-KLK5 (ref HPA014343; Sigma-Aldrich). The technique used was based on indirect immunoperoxidase (kit immPRESS; Vector Laboratories, Burlingame, CA, USA) and revealed with AEC (3-amino-9-éthylcarbazole). Then, semi-quantitative scores were determined according to the staining intensity at the level of *stratum granulosum* and *stratum corneum*. The scores were from 0 to 4 and corresponded with low to high intensity.

2.4.2 | Grading of *stratum corneum* cohesion

After treatment at day 2, 3 explants per donor were fixed in buffered formalin. After the fixation in formalin, the samples were dehydrated and impregnated with paraffin. The samples were then embedded, and sections were made using a microtome. The observation of the general morphology was performed after staining of formalin-fixed and embedded in paraffin sections by hemalun-eosin. The assessment of *stratum corneum* cohesion is directly related to the exfoliation activity of the products.

Based on skin histological sections stained with hemalun-eosin, the anatomopathologist scored the *stratum corneum* cohesion following this grading:

Score 0: no modification of *stratum corneum* cohesion.
Score 1: slight decrease of *stratum corneum* cohesion.
Score 2: moderate decrease of *stratum corneum* cohesion.
Score 3: significant decrease of *stratum corneum* cohesion.
Score 4: highly significant decrease of *stratum corneum* cohesion.

The cohesion assessment was performed on the whole section (10-15 fields at ×40 magnification were analyzed).

2.5 | Clinical investigation

2.5.1 | INCI name of formula used for clinical investigation

AQUA/WATER, CAPRIC/CAPRYLIC TRIGLYCERIDE, CETEARYL WHEAT STRAW GLYCOSIDES, CETEARYL ALCOHOL, ± PROPANEDIOL AND OROBANCHE RAPUM, PHENOXYETHANOL, DIMETHICONE, METHYL PARABEN, PROPYL PARABEN, ETHYL PARABEN, FRAGRANCE, HEXYL CINNAMAL, BUTYLPHENYL METHYLPROPIONAL, CITRONELLOL, ALPHA ISOMETHYL IONONE, HYDROXYISOHEXYL 3-CYCLOHEXENE CARBOXALDEHYDE, SODIUM HYDROXIDE.

2.5.2 | Measurement of skin components by Raman spectroscopy

A double blind, placebo-controlled clinical evaluation was carried out on 19 women (age: 18-50 years old; mean age: 39.5 years) with dry skin (corneometer value below 40 AU). All subjects participating in the study gave their informed consent by signature at the beginning. Measurements were taken after 14 and 28 days of use with the formula, which either did or did not contain *O. rapum* extract at 0.5%. In this study, the parameters studied were the evolution of skin hydration by Raman spectroscopy and the biochemical content evolution of the skin (lipids and proteins).

The set-up included a confocal Raman probe (Horiba Jovin Yvon, Longjumeau, France) coupled with a dispersive Raman spectrograph (Micro HR; Horiba Jobin Yvon). The probe was equipped with a 100× long working distance objective (MPlan FLN Olympus) operating in air with a numerical aperture of 0.9. A piezo-electric device (Physik, Instrumente, Karlsruhe, Germany), allowed to collect Z Raman profiles by assuring axial measurements from the surface down to a defined depth in the skin. The axial resolution of the system was given to about 3 μm by the device manufacturer. A color video camera integrated in the probe enabled visualization of the skin surface. The spectrograph was equipped with a CCD (Coupled Charge Detector) camera (Synapse, Horiba Jobin Yvon, Edison, NJ, USA) of 1024 × 256 elements cooled via the Peltier effect, and an 830 grooves/mm grating enabling coverage of a large spectral range from 550 to 3700 cm^{-1} in a single-shot acquisition with a spectral resolution of about 7 cm^{-1}. The excitation source was a 660 nm laser diode (Ignis Laser Quantum GmbH, Konstanz, Germany). The power at sample was fixed at 30 mW in accordance with protection standards for radiation. The 660 nm excitation was chosen as the optimal compromise between generation of parasitic fluorescence and sensitivity of the CCD camera over the whole spectral range. For skin characterization, the measurement of high wavenumber vibrations is important to access information on water content. Water was identified using band intensity from 3100 to 3600 cm^{-1}, and lipids were identified using band intensity at 1450 cm^{-1}; proteins were identified using Amide I band intensity at 1650 cm^{-1}. Before measurement, the skin surface was gently pressed to ensure a stable contact between

the skin and the probe. Raman profiles were recorded by collecting spectra from the skin surface to 40 μm in depth. The pre-processing of spectral data was performed using Matlab 7.2 (The MathWorks Inc., Natick, MA, USA). Aberrant profiles were excluded by visual inspection of the data. Each non-aberrant profile was submitted to background corrections, which allowed cleanup of the Raman signal of the skin. These background corrections included a notch correction for laser wavelengths removal, followed by a baseline correction using a polynomial function of degree 4, meant to remove the skin fluorescence. Raman spectra were thereafter spatially registered onto a reference spectra (lysopaïne), correcting for instrumental Raman shift, as well as a spatial realignment of the Raman profile. This spatial correction was often necessary since a slight laser defocusing can occur between the probe adjustment on the skin's surface (visually controlled by the laser spot) and the profile acquisition. For this, the *stratum corneum* (SC) surface was located from the Raman profile by determining the Z position corresponding to half of maximum CH intensity (integrated intensity between 2910 and 2965 cm^{-1}). Finally, Raman profiles were spatially smoothed with a 9 mm Savitzky-Golay filter (polynomial function of degree 2) and normalized on the intensity of the entire wavenumber range, with a vectorial function. After these pre-processing steps, corrected data were processed using statistical multivariate analyses.

2.5.3 | Analysis of skin ultrastructure

The evolution of dry skin surface was observed using the OCT tool (Optical Coherence Tomography) and Visioscan® (Courage+Khazaka electronic GmbH, Cologne, Germany). OCT uses light and captures the light reflectance to generate an image. OCT images are two-dimensional images that provide a cross-sectional image of the superficial skin resembling histological images. Therefore, OCT is sometimes referred to as an "optical biopsy," as it aims to provide histologic information non-invasively. OCT imaging systems contain an interferometer illuminated by light. OCT-emitted light is split into two fractions: one fraction is directed to a reference mirror and the other to the tissue. Light reflected back from the mirror and the tissue are recombined and guided to a detector that collects the interference signal and transmits to a computer to generate the image. It offers maximum penetration depth of 1 mm and a field of view of 1.8*1.5 mm. The images are of high resolution with rendering structures up to 3 μm. One measure was taken of each volunteer at each study time (day 0, day 14 and day 28 after *O. rapum* extract or control application).

2.5.4 | Analysis of wrinkles by silicone skin's prints

A simple blind and placebo-controlled clinical evaluation was carried out on 15 women (Age: 35-55 years old; mean age: 43 years ±1) showing clinical signs of aging (wrinkles on crow's feet). All participating subjects gave their informed consent by signature at the beginning of the study. The measurements were taken after 14 and 28 days of use. In this study, the parameters evaluated were the evolution of cutaneous relief using a silicone skin replica technique after

formula application, which either did or did not contain *O. rapum* extract at 0.5%.

Cutaneous relief analysis was done using polymer silicone skin prints (Silflo®), also called replica. Polymer silicone skin prints were taken on crow's feet zones, before product use and at each time of measurement, then analyzed using the Skin Image Analyser® (SIA®). An oblique lighting of 35° casts shadows on the replica surface. These shadows are observed with a digital camera linked to a computer. A 1 cm^2 area was studied. The digitized picture obtained was analyzed in gray levels and allowed different parameters of the skin surface relief to be obtained. The parameters evaluated with the Quanti-Rides® software (Monaderm, Monaco, France) were the total wrinkled surface (in mm^2) and the total wrinkles number. A decrease in these parameters characterizes an anti-wrinkle effect.

2.6 | Metagenomic analysis

2.6.1 | Panel description

A double blind and placebo-controlled clinical evaluation was carried out with 19 women (Age: 18-50 years old; mean age: 39.5) with dry skin (corneometer value below 40 AU). All participating subjects gave their informed consent by signature at the beginning of the study. Metagenomics analysis was performed at day 0 and day 14 after the application to the forearm of products, which either did or did not contain *O. rapum* extract at 0.5%.

2.6.2 | Microbiota sampling and storage

Skin samples of cutaneous microflora were collected from the forearms of healthy volunteers (50 cm^2), by a noninvasive swabbing method, using sterile swabs moistened with a sterile solution of 0.15 mol/L NaCl. Swabs were transferred at −20°C and kept frozen until DNA extraction.

2.6.3 | DNA extraction

DNA extraction was performed using the PowerLyzer® PowerSoil® DNA Isolation Kit (MO BIO Laboratories, Inc., Carlsbad, CA, USA), with the following modifications: The tip of each swab was detached with a sterile surgical blade and transferred to a 1.5 mL tube, with 750 μL of Bead Solution added. The sample biomass was resuspended by stirring and pipetting, and the biological suspension was transferred to a bead beating tube. The remaining steps were performed according to the manufacturer instructions. DNA concentration was determined using the QuBit dsDNA HS fluorometric quantitation kit (Invitrogen) according to the manufacturer instructions.

2.6.4 | 16S rRNA gene sequencing and data analysis

Sequencing was performed with the MiSeq device (Illumina, Inc., San Diego, CA, USA) through a 500-cycle paired-end run, targeting the
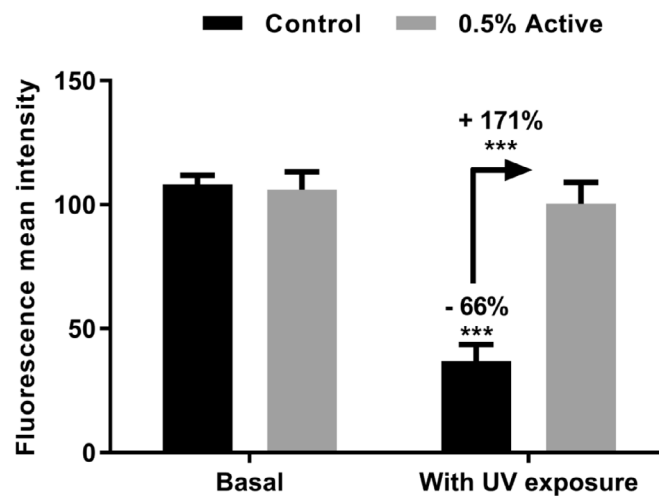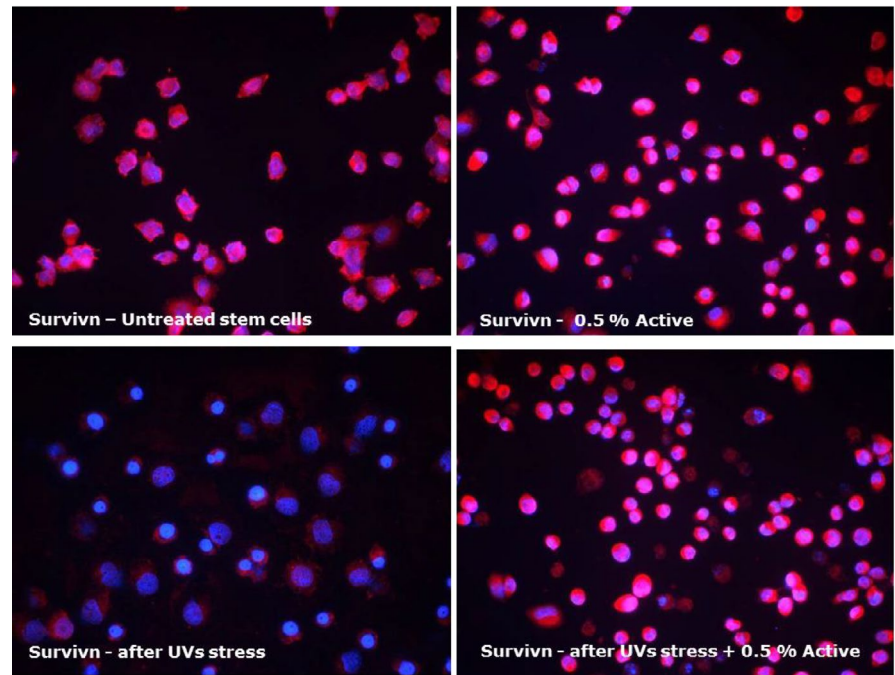
FIGURE 1 Protection of human stem cells against UV exposure via survivin overexpression. ***P value < 0.001 (Active: *Orobanche rapum* extract)

V3V4 16S variable regions using the following primers: 16S-Mi341F forward primer 5'-CCTACGGGNGGCWGCAG-3' and 16S-Mi805R reverse primer 5'-GACTACHVGGGTATCTAATCC-3', producing amplicon of about 460 bp.

PCR1s were performed as follows: 8 μL of template DNA (0.2 ng) was mixed with 5 μL of each reverse and forward primer (1 μmol/L), 5 μL of KAPA (Kapa Biosystems, Inc., Wilmington, MA, USA), HiFi Fidelity Buffer (5×), 0.8 μL of KAPA dNTP Mix (10 mmol/L each), 0.7 μL of RT-PCR grade water (Ambion, Foster City, CA, USA), and 0.6 μL of KAPA HiFi hotstart Taq (1 U/μL), for a total volume of 25 μL. Each amplification was duplicated, and duplicates were pooled after amplification. PCR1 cycles consisted of 95°C for 3 minutes and then 32 cycles of 95°C for 30 seconds, 59°C for 30 seconds, and 72°C for 30 seconds, followed by a final extension at 72°C for 3 minutes, with a BioRad CFX1000 thermocycler. Negative and positive controls were included in all steps to check for contamination. All duplicate

pools were controlled by gel electrophoresis, and amplicons were quantified using fluorometry.

Libraries were then produced following the Illumina® guidelines for 16S metagenomics library preparation. The PCR1 amplicons were purified and controlled using an Agilent 2100 Bioanalyzer (Agilent Technologies). To enable the simultaneous analysis of multiple samples (multiplexing), Nextera® XT indexes (Illumina®) were added during PCR2, with between 15 and 30 ng of PCR1 amplicons. PCR2 cycles consisted of 94°C for 1 minute and then 12 cycles of 94°C for 60 seconds, 65°C for 60 seconds, and 72°C for 60 seconds, followed by a final extension at 72°C for 10 minutes. Indexed libraries were purified, quantified, and controlled using an Agilent 2100 Bioanalyzer. Validated indexed libraries were pooled in order to obtain an equimolar mixture.

The run (500 cycles) was achieved on a MiSeq sequencer (Illumina®) using the MiSeq Reagent Kit v3 (600 cycles) (Illumina).
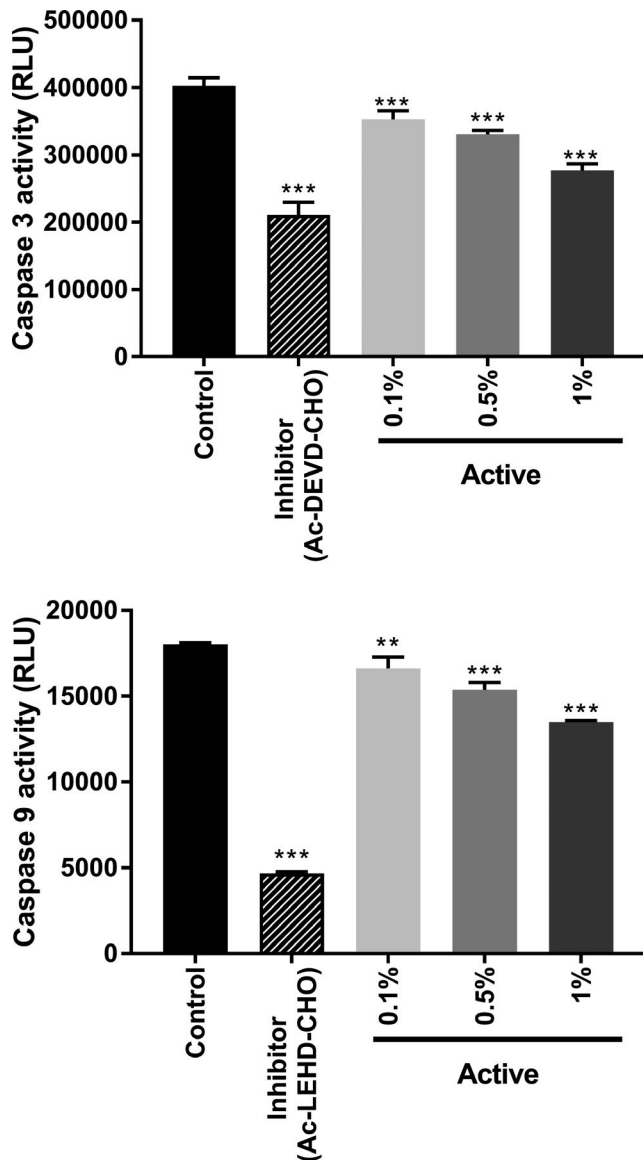
FIGURE 2 Protection of human stem cells from apoptosis through inhibition of caspase 3 and caspase 9 activities. **P value < 0.01; ***P value < 0.001 (Active: *Orobanche rapum* extract)

The sequencing run produced an output of 25 million paired-end reads of 250 bases, that is, up to 6 gigabases. The libraries and the MiSeq run were performed by Givaudan, at the GeT-PlaGe platform (INRA, Auzeville, France).

After MiSeq run, raw data sequences were de-multiplexed and quality-checked to remove all reads with ambiguous bases. Indexes and primer sequences were removed with cutadapt (v1.9—https://cutadapt.readthedocs.io/en/stable/index.html), and reads with fastq score lower than 28 were trimmed. The paired-sequences were then treated using in-house pipeline to remove chimeras and reads with PCR errors and to split sequences into Operational Taxonomic Units (OTU) at a 1% dissimilarity level. Good quality binned paired-sequences were mapped to the SILVA SSU Ref NR database (Release 123; https://www.arb-silva.de/) for taxonomic assignation. Data were then normalized and compared using White's non-parametric test.[21]

3 | RESULTS

3.1 | Impact on skin rejuvenation

We first studied the impact of the selected plant extract on human stem cells after UV exposure targeting the expression of survivin. We demonstrated that human stem cells are very sensitive to UV exposure, as observed by the drastic decrease of survivin expression after exposure. We can suppose that UV disrupted the stem cell properties and their capacity to replicate themselves through the decrease of survivin expression, but not their cell viability as observed by the nucleus staining (Figure 1). A pre-incubation with *O. rapum* extract at 0.5% induced a relevant protection against UV exposure as observed by the restoration of survivin expression (Figure 1). Following the restoration of survivin expression, we were able to evidence the capacity of the extract to protect the stem cells against UV exposure. In order to know whether the tested extract could directly influence the caspase activity through survivin expression, we measured the caspase 3 and caspase 9 activities (Figure 2): A significant and dose-dependent inhibition of caspase 3 and caspase 9 was demonstrated, with a maximal effect at 1% of *O. rapum* extract. These results demonstrated that *O. rapum* extract is able to directly inhibit the caspase 3 and 9 which are two key caspases involved in the apoptosis mechanism.

3.2 | Impact on epidermal differentiation

We then evaluated the impact of *O. rapum* extract on the epidermal differentiation process. In the first study, we worked on skin without lipids mediated by tape-stripping in order to study the benefit of our plant extract in a disrupted barrier function model. As visible in Figure 3, the RHE used presents a very low expression of filaggrin, involucrin, and loricrin, which are terminal epidermal differentiation markers involved in barrier function. The decrease of their expression demonstrated a disruption of barrier function in the used model (Figure 3). The efficacy of *O. rapum* extract to restore the barrier function was evaluated after 72 hours of application with formulated products vs placebo and in comparison with a reference molecule, hyaluronic acid. The placebo did not show any effect on the expression of filaggrin, involucrin, and loricrin, whereas the formula containing *O. rapum* extract at 0.5% evidenced a relevant increase of their expressions after 72 hours of application. The fluorescence quantification demonstrated that the product containing *O. rapum* extract at 0.5% significantly restored the expression of involucrin and loricrin and improved the filaggrin expression after 72 hours (Figure 3). The effects obtained were superior to those from the reference molecule used in this study, hyaluronic acid. In the second study, we worked on RHE treated with a cytokines mixture in order to induce a decrease in filaggrin expression and thus, mimic the barrier disruption. As seen in Figure 4, the barrier alteration with cytokines induced a significant decrease of total ceramides expression, the lipids involved in skin impermeability. This shows that when skin barrier function is altered, there is a loss of ceramides, but their level
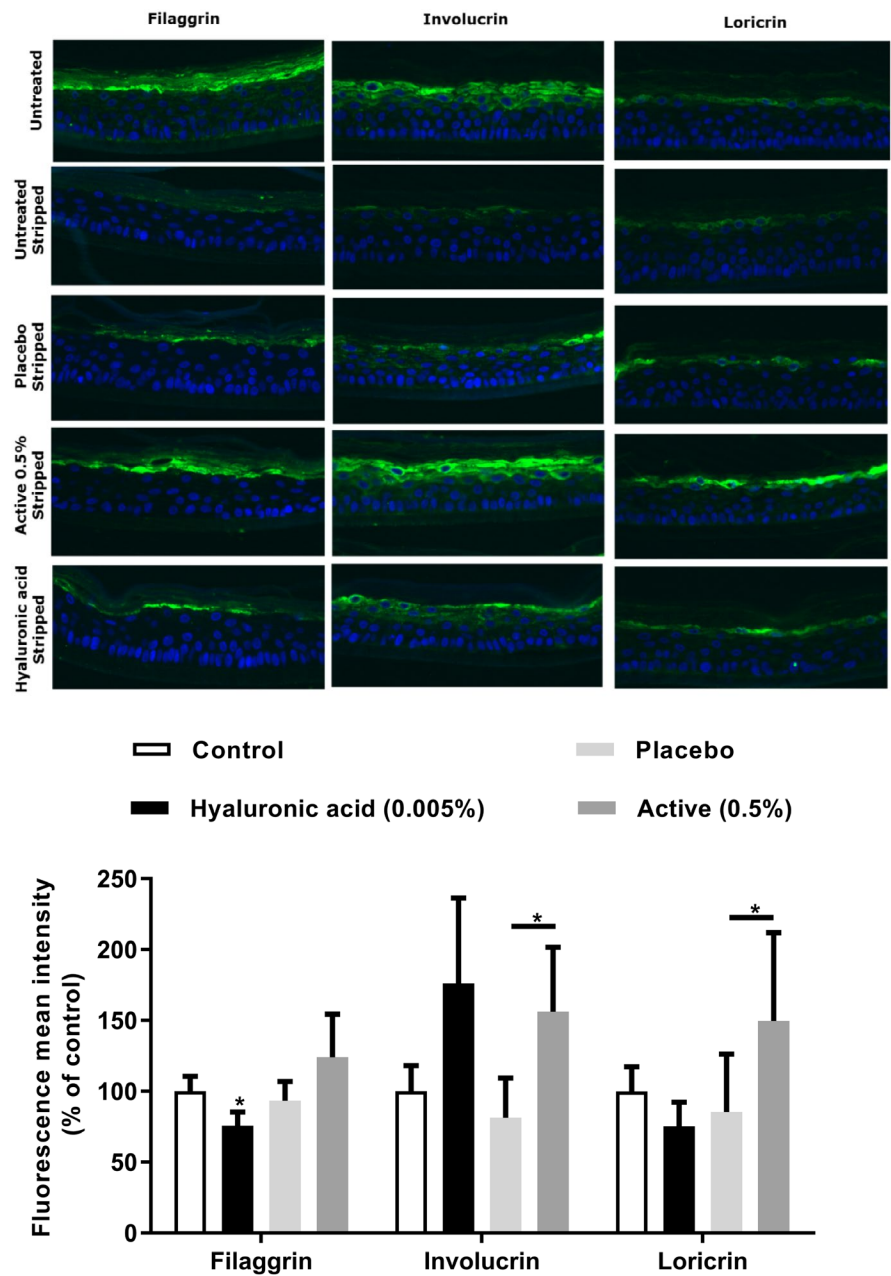
FIGURE 3 Improvement of skin renewal process and enhancement of skin barrier function by overexpression of cell differentiation markers in RHE without lipids (stripping). *P value < 0.05 (Active: *Orobanche rapum* extract)

is nearly restored when *O. rapum* extract is added to cytokines treatment (Figure 4). A focus was placed on fatty acid chain length when stimulated by *O. rapum* extract and an analysis by LC/MS evidenced that cytokines induced a decrease in their chain length, whereas there was a significant increase of *O. rapum* extract (Figure 5).

3.3 | Impact on desquamation

The process of desquamation was then studied with KLK5, a key factor in the desquamation process, and we studied its expression in human skin explants kept in survival and topically treated for 2 days with *O. rapum* extract vs placebo. As seen in Figure 6, the untreated skin presents a low expression of KLK5 in *stratum granulosum* and *stratum corneum*. The same observation can be made for

skin treated with placebo. Incubation for two days with *O. rapum* extract at 0.5% induced a significant increase of KLK5 expression, suggesting that the active has a stimulating effect on desquamation. To confirm this, a scorage was made on the *stratum corneum* cohesion (Figure 7) showing a significant decrease of the upper layer cohesion. Results of this scorage are consistent with the appearance of *stratum corneum* on the skin section pictures, which appear to be deconstructed and less cohesive than with skin control and placebo treated skin.

3.4 | Clinical study

To go further at the clinical level, we carried out a clinical study using Raman spectroscopy in order to analyze the effect of the extract
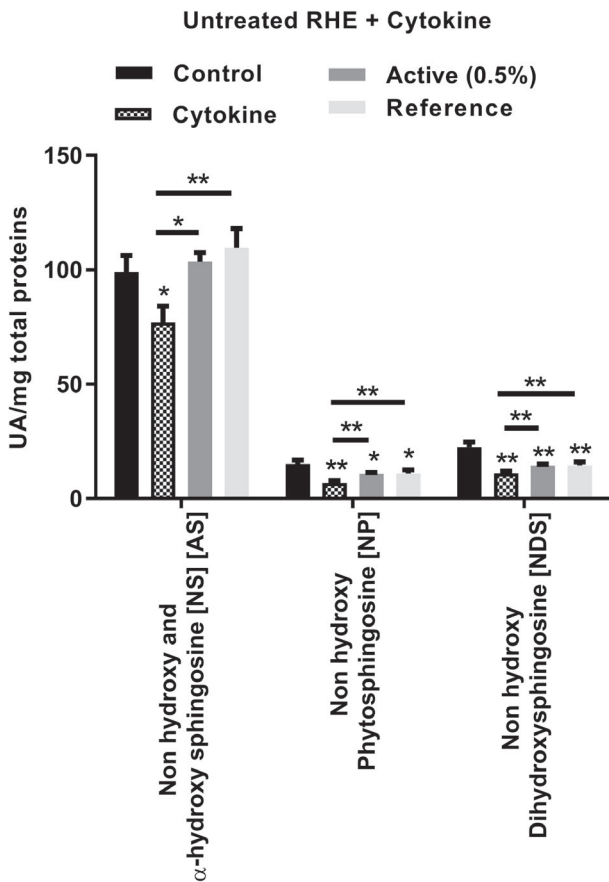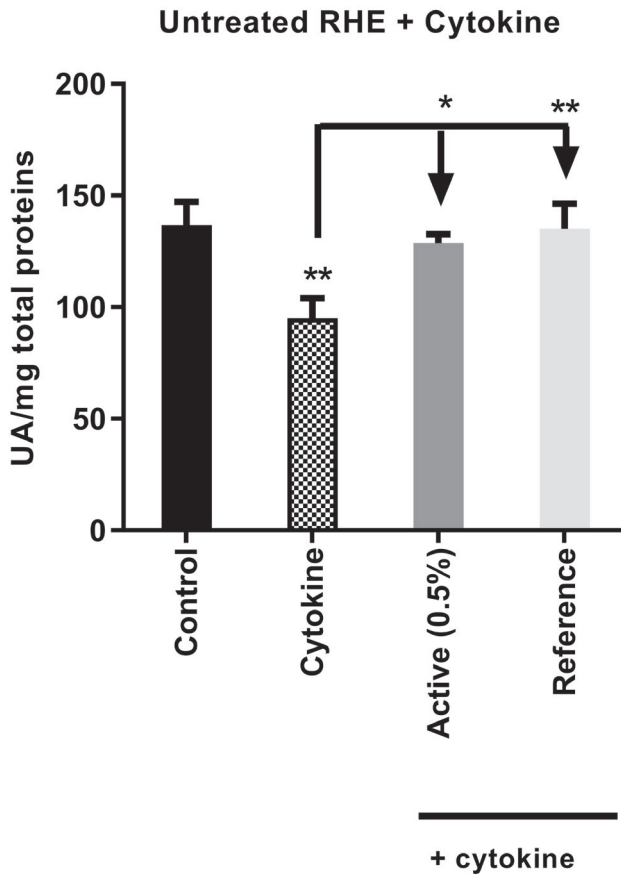
Untreated RHE + Cytokine

on skin composition at in vivo level. The volunteers applied products which either did or did not contain *O. rapum* extract on the forearm area for 28 days in two daily applications. We analyzed the total water, lipid, and protein contents after 14 and 28 days of treatment. We observed a significant increase in total water content after 14 and 28 days of both products (Figure 8). However, the product containing *O. rapum* extract at 0.5% showed better results than placebo with a significant difference after 28 days of application. Similar results were obtained on lipid and protein contents, showing a significant improvement of their contents with the product containing *O. rapum* extract at 0.5% relative to placebo (Figure 8). We performed Optical Coherence Tomography analysis in order to observe the ultrastructure of the skin including epidermis, dermo-epidermal junction, and dermis structure. Using OCT, the younger the skin is, with a properly organized dermis, the more the signal is intense. In contrast, a weak signal is a characteristic of an old skin and a disrupted dermis organization. We used this method to observe the potential skin renewal process activation with *O. rapum* extract application after 28 days of application. Our results clearly showed that the product containing *O. rapum* extract at 0.5% displayed a better organization of the skin with more intense signal in OCT in comparison with placebo results (Figure 9).

We performed a second clinical study to prove skin rejuvenation activation with the *O. rapum* extract. In this study, we worked on volunteers presenting wrinkles at crow's feet area where they
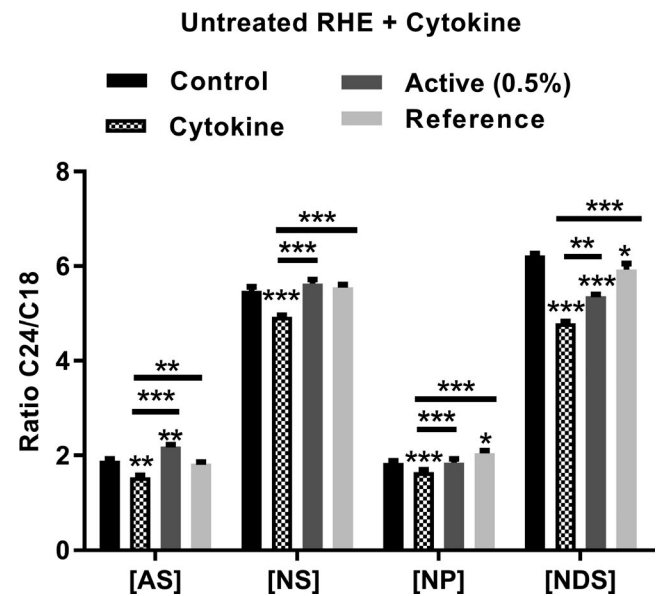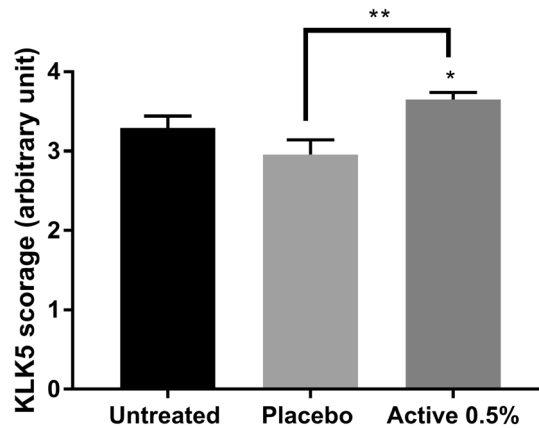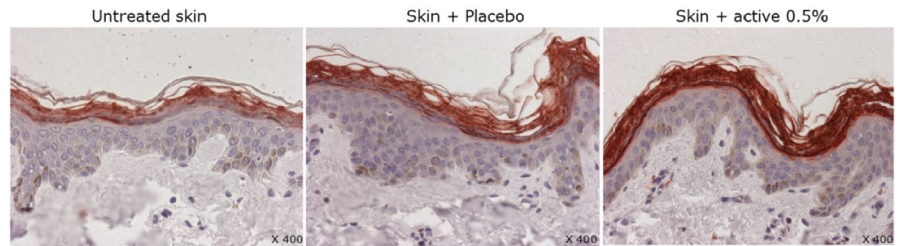
FIGURE 6 Increase of KLK5 expression in the presence of *Orobanche rapum* extract (Active). KLK5 is a protein responsible for *stratum corneum* desquamation. *P value < 0.5; **P value < 0.01

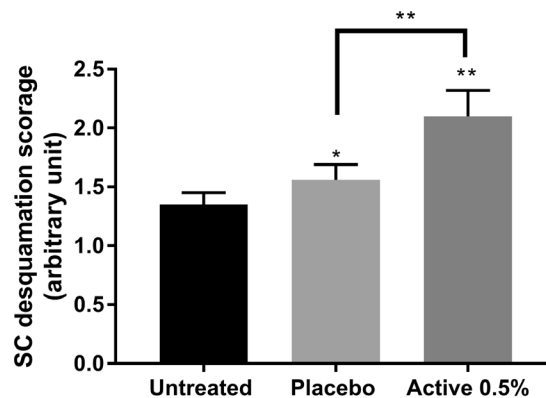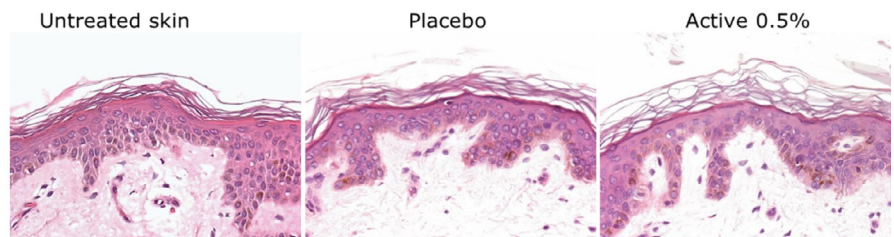**FIGURE 7** Activation of *stratum corneum* desquamation confirmed by a scorage of *stratum corneum* cohesion. *P value < 0.5; **P value < 0.01 (Active: *Orobanche rapum* extract)

applied the products which either did or did not contain *O. rapum* extract at 0.5% with two daily applications for 28 days. We observed a significant reduction of total wrinkled area −28.5% after 14 days of treatment with the product containing 0.5% of *O. rapum* extract, while the placebo had no effect (Figure 10). After 28 days, we demonstrated that the product containing 0.5% of *O. rapum* extract significantly decreased the number of wrinkles and the total wrinkled area with −12% and −31%, respectively (Figure 10). These effects were significantly relative to day 0 and placebo (Figure 10).

We finally performed metagenomics analysis in order to observe the impact of the product, which either did or did not contain *O. rapum* extract at 0.5%, on skin microbiota after 14 days of application on forearm.

After 14 days of treatment, the microbiota evolved differently in reaction to the treatment. At the phylum level, when treated with formula without extract, a significant increase of *Firmicutes* is observed from 26.2% (day 0) to 37.0% (day 14). In the same condition, the other phyla stay stable (Figure 11). After 14 days of treatment with formula containing 0.5% of *O. rapum* extract, all phyla stay
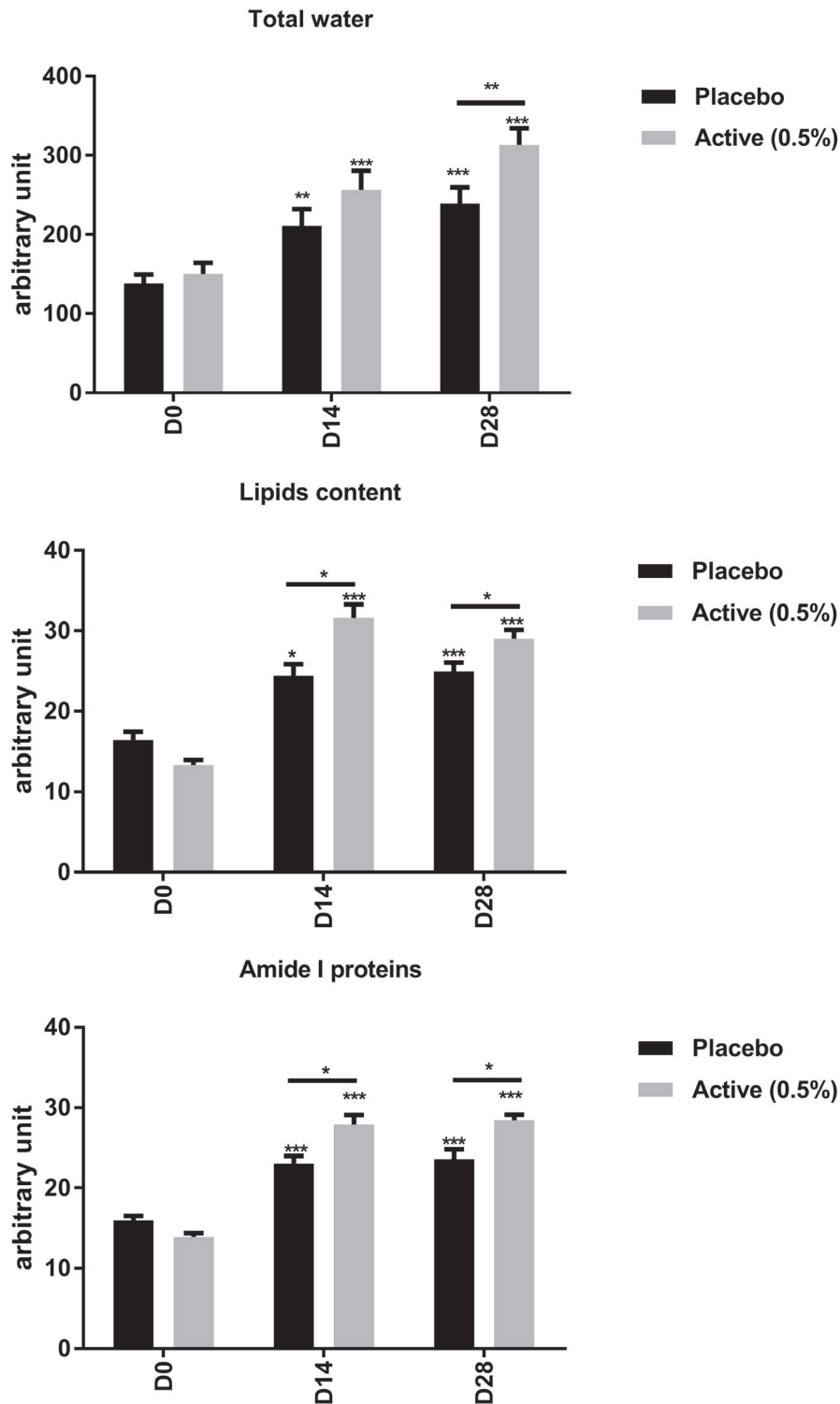
FIGURE 8 Improvement of *stratum corneum* content with *Orobanche rapum* extract (Active), which induces an increase of lipids, amide I proteins and water. *P value < 0.5; **P value < 0.01; ***P value < 0.001

stable, even the *Firmicutes* (Figure 11). At the genus level, among the most abundant genera (>1%) *Finegoldia* is the only genus significantly impacted by the active (Table 1). During treatment with *O. rapum* extract, the average relative abundance of *Finegoldia* significantly decreased from 3.1% (day 0) to 1.3% (day 14) (Figure 12). Without *O. rapum* extract (formula only, see Figure 12 and Table 1), *Finegoldia* stays stable. Thus, the active inhibits growth of the opportunistic pathogen *Finegoldia*.

4 | DISCUSSION

During the skin rejuvenation, stem cells play an active role, given their capacity to regenerate skin tissue. A drastic slowdown of epidermal turnover was observed with age, this being correlated with a significant decrease of stem cells and their property. In the first part of this work, we studied the impact of our plant extract on human stem cells after UV exposure targeting the expression of survivin. It is a stem cell biomarker
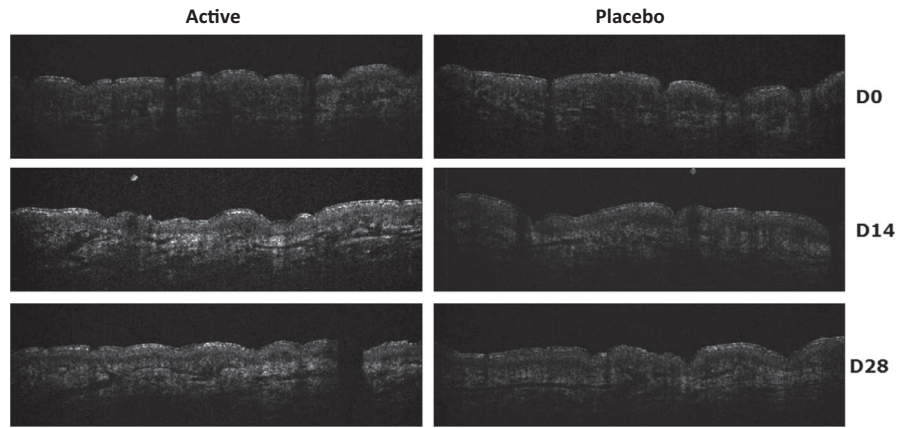
FIGURE 9 Optical Coherence Tomography pictures of skin at the clinical level showing the enhancement of dermis organization with *Orobanche rapum* extract (Active), leading to a younger aspect for skin

|	Parameters	Active			Placebo			Student t-test versus placebo (p)
		Δ Mean +/- SEM	Δ % (mean)	Student t-test versus D0 (p)	Δ Mean +/- SEM	Δ % (mean)	Student t-test versus D0 (p)	
D14-D0	Total wrinkles (Number)	-3.7 ± 4.3	-3.6%	0.402	7.9 ± 5.0	10.8%	0,136	**0.044**
	Total wrinkled area [mm²]	-5.2 ± 1.6	-28.5%	**0.006**	0.2 ± 1.7	1.4%	0,911	**0.014**
D28-D0	Total wrinkles (Number)	-12.1 ± 5.4	-11.9%	**0.041**	8.9 ± 4.7	12.2%	0.082	**0.003**
	Total wrinkled area [mm²]	-5.6 ± 2.1	-30.6%	**0.017**	-2.5 ± 1.5	-18.4%	0.126	0.119
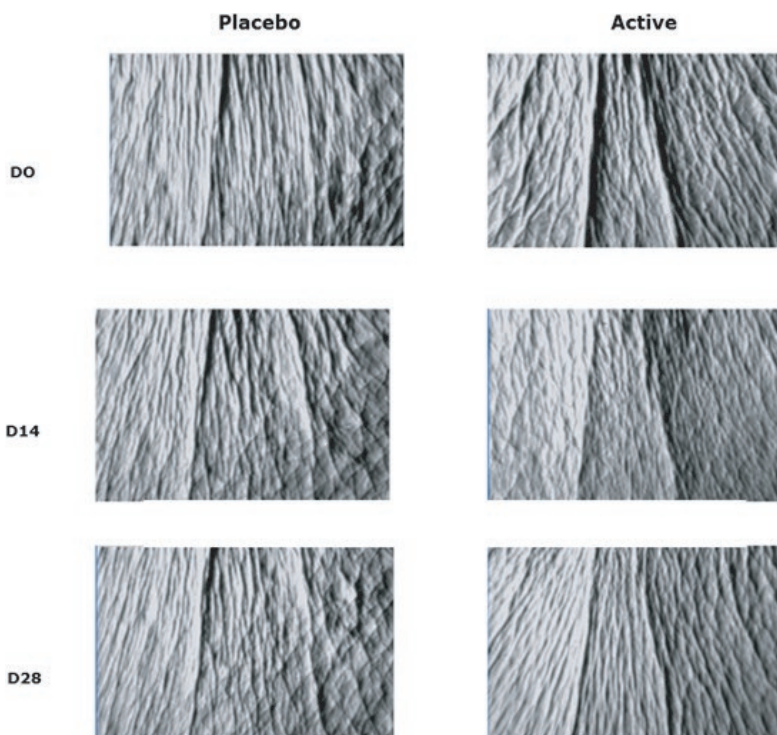
FIGURE 10 Number of wrinkles and their area are significantly reduced for skin treated with *Orobanche rapum* extract

Vehicle - Phyla distribution (>0,1%)

Active - Phyla distribution (>0.1%)

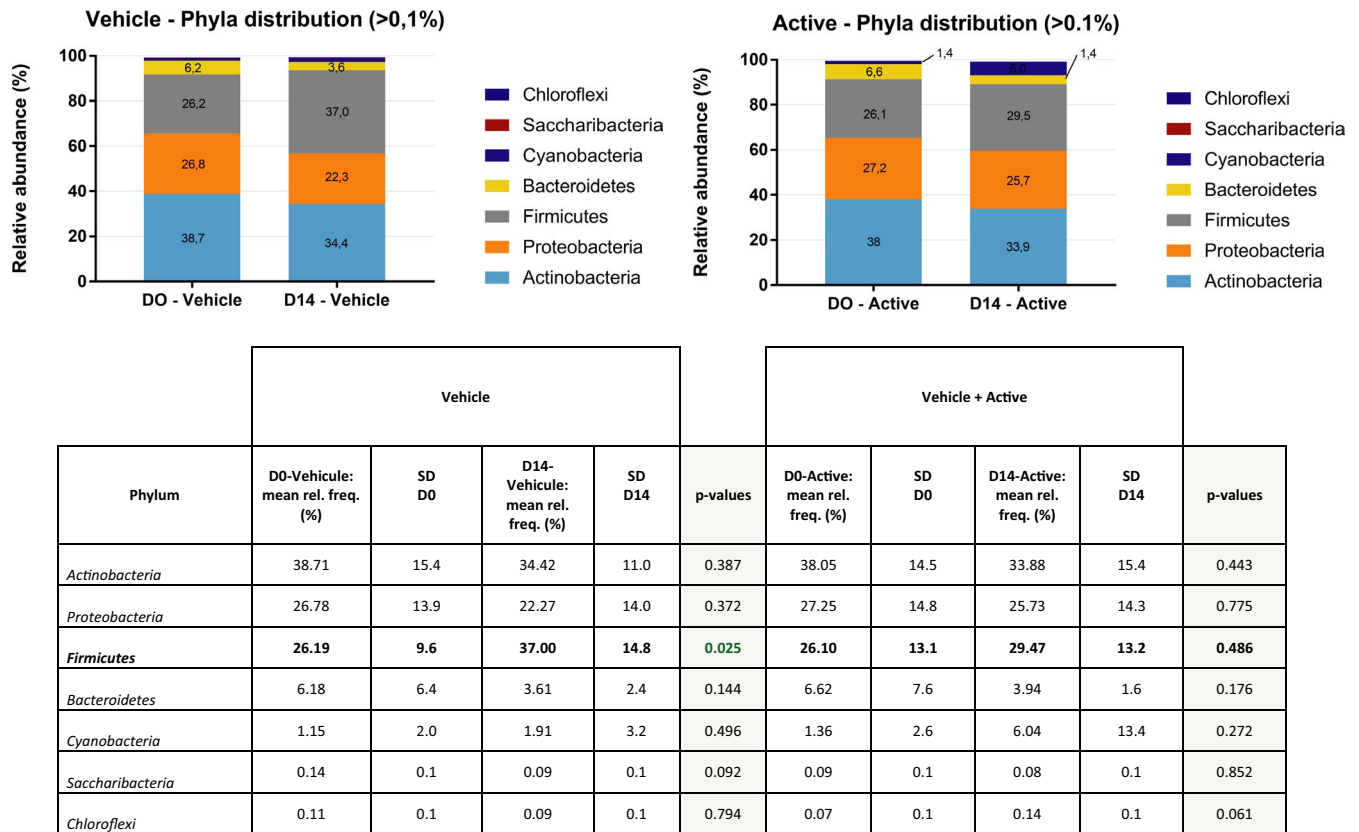|	Vehicle					Vehicle + Active				
Phylum	D0-Vehicule: mean rel. freq. (%)	SD D0	D14-Vehicule: mean rel. freq. (%)	SD D14	p-values	D0-Active: mean rel. freq. (%)	SD D0	D14-Active: mean rel. freq. (%)	SD D14	p-values
Actinobacteria	38.71	15.4	34.42	11.0	0.387	38.05	14.5	33.88	15.4	0.443
Proteobacteria	26.78	13.9	22.27	14.0	0.372	27.25	14.8	25.73	14.3	0.775
Firmicutes	**26.19**	**9.6**	**37.00**	**14.8**	**0.025**	**26.10**	**13.1**	**29.47**	**13.2**	**0.486**
Bacteroidetes	6.18	6.4	3.61	2.4	0.144	6.62	7.6	3.94	1.6	0.176
Cyanobacteria	1.15	2.0	1.91	3.2	0.496	1.36	2.6	6.04	13.4	0.272
Saccharibacteria	0.14	0.1	0.09	0.1	0.092	0.09	0.1	0.08	0.1	0.852
Chloroflexi	0.11	0.1	0.09	0.1	0.794	0.07	0.1	0.14	0.1	0.061

FIGURE 11 Relative quantity of different phyla composing skin microbiota is kept stable with *Orobanche rapum* extract, showing its ability to maintain the skin microbiota balance

that presents two different biological functions according to cell location. In nucleus, survivin is involved in the control of cell division correlated with stem cell status. In the cytoplasm, survivin plays an active anti-apoptotic response against the UV via caspase 3 and 9 inhibition.

Our data evidenced that *O. rapum* is able to protect and maintain the pool of stem cells in the skin *via* overexpression of survivin, and its impact on caspases 3 and 9 inhibition was clearly demonstrated. As a long-term consequence, *O. rapum* could significantly increase the rejuvenation power of the skin.

In the skin renewal process, stem cells regularly generate new precursor cells, highly proliferative cells able to enter the epidermal cell differentiation program to restore the skin. We evaluated the impact of *O. rapum* extract on the epidermal differentiation process working on a disrupted barrier function model. The fluorescence quantification demonstrated that the product containing *O. rapum* extract at 0.5% significantly restored the expression of involucrin and loricrin and improved the filaggrin expression after 72 hours (Figure 3). These results confirmed that *O. rapum* extract is able to improve the skin differentiation process, restoring efficient skin barrier function. After addressing the skin renewal process, we turned toward lipid production on the epidermis, which is very important for skin permeability and directly linked to epidermal differentiation. The differentiated keratinocytes transform themselves into corneocytes. Corneocytes are the cells able to release specific lipids which create the skin's cement, allowing for impermeability. We worked on RHE treated with a cytokines mixture

in order to induce a decrease in filaggrin expression and thus, mimic the barrier disruption. Results shown that *O. rapum* extract stimulates the production of total ceramides with a long chain length, leading to the improvement of orthorhombic lipid organization, and so conferring a restoration of the barrier function. All these data confirm that *O. rapum* extract activates the epidermal differentiation up to lipid synthesis by corneocytes and so ensures the skin barrier function.

The final step of skin renewal is the process of desquamation. After proliferation of human stem cells leading to the epidermal differentiation process, all epidermal layers are renewed and replace the previous ones. Below the ancient *stratum corneum*, a new *stratum granulosum* is formed, composed of lamellar bodies containing kallikrein 5 (KLK5). Kallikrein 5 is a serine protease activated by the acidic environment of the *stratum corneum* extracellular space and specialized in the cleavage of corneodesmosomal components. KLK5 is a key factor in the desquamation process, and its expression was increased by *O. rapum* extract at 0.5%, suggesting that the active has a stimulating effect on desquamation. A scorage made on the *stratum corneum* cohesion confirmed this last is deconstructed and less cohesive than with skin control and placebo treated skin. These data suggest that *O. rapum* extract could stimulate skin renewal up to the process of desquamation.

First, we demonstrated at in vitro and ex vivo the extent to which *O. rapum* extract is able to improve the skin composition and epidermal renewal process. Our clinical study with Raman spectroscopy evidenced that *O. rapum* significantly improved the skin composition

TABLE 1 Relative quantity of genus *Finegoldia* measured on skin is significantly lower with *Orobanche rapum* extract (Active)

Genus	Active 0.5%					Placebo				
	D0-Active: mean rel. freq. (%)	SD D0	D14-Active: mean rel. freq. (%)	SD D14	P-value	D0-Vehicle: mean rel. Freq. (%)	SD D0	D14-Vehicle: mean rel. Freq. (%)	SD D14	P-value
Finegoldia	3.1	3.7	**1.3***	1.1	0.043	1.9	1.5	2.1	2.3	0.741

*The bold values indicate the relative quantity of genus Finegoldia measured on skin (in %).
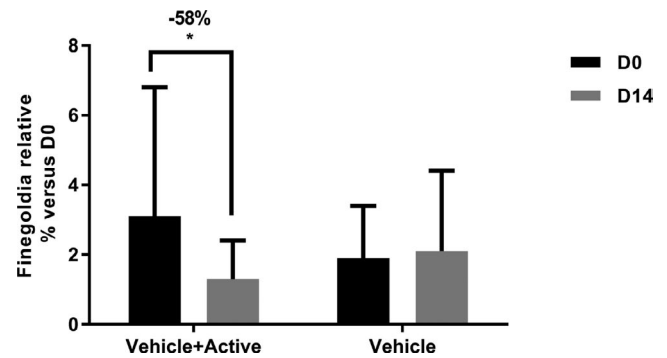
FIGURE 12 Pathogenic genus *Finegoldia* is significantly decreased in presence of *Orobanche rapum* extract (Active), proving its protective effect on skin. *P value < 0.5%

in vivo after 28 days of application by increasing water, lipid, and protein contents (Figure 8). Overall, these results suggest a global skin improvement and rejuvenation. An additional study by OCT analysis on the same panel confirmed that *O. rapum* extract activated the skin renewal process and promoted skin rejuvenation with younger aspect (Figure 9). We also evidenced that *O. rapum* extract at 0.5% induced significant anti-aging efficacy at the skin surface by a significant decrease of the number of wrinkles and the total wrinkles area, due to its rejuvenation activity linked to the activation of skin renewal (Figure 10).

We previously demonstrated that *O. rapum* extract was able to reactivate the skin renewal process leading to skin composition improvement and wrinkle reduction. These effects could influence the skin surface and modify skin microbiota. We performed metagenomics analysis and observed that *O. rapum* extract stabilizes microbiota and maintains the essential balance of skin microflora (Figure 11). We also noticed a significant impact on the genus *Finegoldia* (Table 1). *Finegoldia magna* is the only characterized species among the *Finegoldia* genus. This species is a normal inhabitant of human skin and is the most frequently Gram positive cocci isolated from infected lesions.[22] *Finegoldia magna* can be involved in mono- and poly-microbial infection of skin, bones, heart, and meninges.[23] A case of toxic shock syndrome caused by *F magna* has also been reported by Rosenthal et al.[17] Thus, *O. rapum* extract inhibits growth of the opportunistic pathogen *Finegoldia*.

5 | CONCLUSION

In this study, we first demonstrated in vitro how *O. rapum* extract impacts skin renewal at its origin by protecting skin stem cells, enhancing the expression of survivin and inhibiting activation of caspases 3 and 9. This protection leads to the improvement of in vitro epidermal differentiation up to the upper step. This claim was proven by staining terminal differentiation proteins like filaggrin, involucrin, and loricrin on a reconstructed human epidermis (RHE). Epidermis impermeability restoration after a barrier disruption was also evidenced with *O. rapum* extract. This restoration of the barrier function was explained by the analysis of ceramide content by GC/MS The analysis showed an increase of ceramide content and demonstrated

that the ceramides were composed of long chains. An increase in the number of long chain ceramides allows for orthorhombic lipid organization, improving water holding and enhancing skin barrier function. We proved that *O. rapum* extract completed this skin renewal process up to the process of desquamation, by increasing the kallikrein 5 expression and so inducing a loss of *stratum corneum* cohesion. At the clinical level, it has been proven that this process of skin renewal leads to a rejuvenating effect by smoothing wrinkles. Despite all these effects on biological skin activity, *O. rapum* extract showed that it was able to maintain skin microbiota balance by keeping the *Stratum microbium*™ composition safe while inducing a slight decrease of potentially pathogenic bacteria *Finegoldia*. Givaudan has developed a new plant extract able to induce skin renewal and rejuvenation while protecting its best ally, the *Stratum microbium*™.

ACKNOWLEDGMENTS

ORCID

Marie Meunier iD http://orcid.org/0000-0003-2925-9094

REFERENCES

1. Fuchs E. Skin stem cells: rising to the surface. *J Cell Biol.* 2008;180:273-284. https://doi.org/10.1083/jcb.200708185.
2. Martin MT, Vulin A, Hendry JH. Human epidermal stem cells: role in adverse skin reactions and carcinogenesis from radiation. *Mutat Res.* 2016;770:349-368. https://doi.org/10.1016/j.mrrev.2016.08.004.
3. Moore KA, Lemischka IR. Stem cells and their niches. *Science.* 2006;311:7.
4. Panich U, Sittithumcharee G, Rathviboon N, Jirawatnotai S. Ultraviolet radiation-induced skin aging: the role of DNA damage and oxidative stress in epidermal stem cell damage mediated skin aging. *Stem Cells Int.* 2016;2016:1-14. https://doi.org/10.1155/2016/7370642.
5. Liu L, Rando TA. Manifestations and mechanisms of stem cell aging. *J Cell Biol.* 2011;193:257-266. https://doi.org/10.1083/jcb.201010131.
6. Zouboulis CC, Adjaye J, Akamatsu H, Moe-Behrens G, Niemann C. Human skin stem cells and the ageing process. *Exp Gerontol.* 2008;43:986-997. https://doi.org/10.1016/j.exger.2008.09.001.
7. Dallaglio K, Petrachi T, Marconi A, et al. Expression of nuclear survivin in normal skin and squamous cell carcinoma: a possible role in tumour invasion. *Br J Cancer.* 2013;110:199-207. https://doi.org/10.1038/bjc.2013.697.
8. Watt FM. Epidermal stem cells: markers, patterning and the control of stem cell fate. *Philos Trans R Soc B Biol Sci.* 1998;353:831-837. https://doi.org/10.1098/rstb.1998.0247.
9. Alberts B, Johnson A, Lewis J. *Molecular Biology of the Cell*, 4th edn. New York, NY: Garland Science; 2002.
10. Wikramanayake TC, Stojadinovic O, Tomic-Canic M. Epidermal differentiation in barrier maintenance and wound healing. *Adv Wound Care.* 2014;3:272-280. https://doi.org/10.1089/wound.2013.0503.
11. Wertz PW, Miethke MC, Long SA, Strauss JS, Downing DT. The composition of the ceramides from human stratum corneum and from comedones. *J Invest Dermatol.* 1985;84:410-412. https://doi.org/10.1111/1523-1747.ep12265510.
12. Menon GK, Kollias N, Doukas AG. Ultrastructural evidence of stratum corneum permeabilization induced by photomechanical waves. *J Invest Dermat.* 2003;121:104-109. https://doi.org/10.1046/j.1523-1747.2003.12302.x.
13. Yoon H, Laxmikanthan G, Lee J et al. Activation profiles and regulatory cascades of the human Kallikrein-related peptidase. *J Invest Dermatol.* 2007;282:31852-31864.
14. Borgono CA, Michael IP, Komatsu N, et al. A potential role for multiple tissue kallikrein serine proteases in epidermal desquamation. *J Biol Chem.* 2006;282:3640-3652. https://doi.org/10.1074/jbc.m607567200.
15. Nakatsuji T, Chiang H-I, Jiang SB, Nagarajan H, Zengler K, Gallo RL. The microbiome extends to subepidermal compartments of normal skin. *Nat Commun.* 2013;4(1):1431. https://doi.org/10.1038/ncomms2441.
16. Nakamizo S, Egawa G, Honda T, Nakajima S, Belkaid Y, Kabashima K. Commensal bacteria and cutaneous immunity. *Semin Immunopathol.* 2015;37(1):73-80.
17. Rosenthal M, Goldberg D, Aiello A, Larson E, Foxman B. Skin microbiota: microbial community structure and its potential association with health and disease. *Infect Genet Evol.* 2011;11:839-848. https://doi.org/10.1016/j.meegid.2011.03.022.
18. Wallen-Russell C, Wallen-Russell S. Meta analysis of skin microbiome: new link between skin microbiota diversity and skin health with proposal to use this as a future mechanism to determine whether cosmetic products damage the skin. *Cosmetics.* 2017;4:14. https://doi.org/10.3390/cosmetics4020014.
19. Zapata HJ, Quagliarello VJ. The microbiota and microbiome in aging: potential implications in health and age-related diseases. *J Am Geriatr Soc.* 2015;63:776-781. https://doi.org/10.1111/jgs.13310.
20. Andary C, Wylde R, Laffite C, Privat G, Winternitz F. Structures of verbascoside and orobanchoside, caffeic acid sugar esters from *Orobanche rapum-genistae*. *Phytochemistry.* 1982;21:1123-1127. https://doi.org/10.1016/s0031-9422(00)82429-2.
21. White JR, Nagarajan N, Pop M. Statistical methods for detecting differentially abundant features in clinical metagenomic samples. *PLoS Computational Biology.* 2009;5:e1000352. https://doi.org/10.1371/journal.pcbi.1000352
22. Murphy E, Janulczyk R, Karlsson C, Mörgelin M, Frick I-M. Identification of pili on the surface of *Finegoldia magna* - A Gram - positive anaerobic cocci. *Anaerobe.* 2014;27:40-49.
23. Murphy E, Frick I-M. Gram-positive anaerobic cocci-commensals and opportunistic pathogens. *FEMS Microbiol Rev.* 2013;37:520-553.